Preparation and Characterization of Poly(2-chloroaniline)/SiO_2 Nanocomposite via Oxidative Polymerization: Comparative UV–Vis Studies into Different Solvents of Poly(2-chloroaniline) and Poly(2-chloroaniline)/SiO_2

Ayşegül Gök,[1] Songül Şen[2]

[1]*Department of Chemistry, Faculty of Science and Arts, Süleyman Demirel University, 32260 Isparta, Turkey*
[2]*Research Center, Süleyman Demirel University, 32260 Isparta, Turkey*

Received 21 July 2005; revised 28 January 2006; accepted 17 February 2006
DOI 10.1002/app.24266
Published online in Wiley InterScience (www.interscience.wiley.com).

ABSTRACT: Poly(2-chloroaniline)/silica (P2ClAn)/SiO_2 nanocomposites have been chemically prepared by oxidative polymerization of 2-chloroaniline in acidic medium containing SiO_2. The prepared composites were characterized by FTIR, UV–vis, TGA, XRD, SEM, ESEM, conductivity, and magnetic susceptibility. The incorporation of P2ClAn in composites was endorsed by FTIR studies. The effect of the solution concentration of P2ClAn and P2ClAn/SiO_2 prepared in protonated, deprotonated, and reprotonated structures on the UV–vis spectra was investigated into three different solvents (DMF, NMP, and H_2SO_4). In all forms, the oxidation state of P2ClAn and P2ClAn/SiO_2 composite increased with increasing concentration of the testing solution into H_2SO_4. Thermogravimetric study exhibited that the composite has a higher thermal stability than P2ClAn. XRD measurement of the composite revealed that the crystal structure of incorporated SiO_2 undergone a distortion and converted into amorphous. Thus, the XRD pattern of P2ClAn was predominant. SEM analysis results revealed interesting morphological features for the composites converted to different forms and confirmed the formation of monodispersed composite particles. ESEM image of P2ClAn/SiO_2 has particle diameter of less than 1 μm. The conductivity of P2ClAn and P2ClAn/SiO_2 was measured by four-probe technique. Magnetic susceptibility measurements revealed that the composite has a paramagnetic properties. © 2006 Wiley Periodicals, Inc. J Appl Polym Sci 102: 935–943, 2006

Key words: conducting polymer; morphology; UV-visible spectroscopy; poly(2-chloroaniline); SiO_2

INTRODUCTION

Electrically conducting polymers are novel class of synthetic metals that combine the chemical and mechanical properties of polymers with the electronic properties of metals and semiconductors.[1] Polyaniline (PAni) is one of the most intensively conducting polymers studied during the last decade. It is highly conducting, easy to synthesize both chemically as a green powder or electrochemically as a film.[2–4] The chemical method has a great importance since it is very feasible route for the mass production of PAni.

Composites of conjugated polymers are interesting because of their potential for combining properties that are difficult to attain separately with individual components. Nanocomposites based on conducting polymer and transition metal oxides have been intensively investigated during recent years due to their potential applications as electrode material in lithium batteries.[5] These composites were prepared by polymerization of the monomers in the presence of dispersed oxide. Three methods for deriving such nanocomposites are known.[6] The first one includes the intercalation of the monomers into the host matrix followed by their polymerization due to the presence of an external oxidizing agent. In the second method, the redox properties of the host (metal oxide) ensure *in situ* polymerization as well as intercalation of polymer macromolecules inside the host particles. Several inorganic nanoparticles such as CdS and CuS,[7] clay,[8] maghemite,[9] MnO_2,[10] TiO_2,[11] and ZrO_2[12] had been used for the conductive PAni nanocomposites.

It is well known that PAni has a very strong pH sensitivity, which is deprotonated on a reversible acid-deprotonated reaction between the half-oxidized emeraldine deprotonated (EB) and the emeraldine salt (ES) form of PAni. The emeraldine deprotonated form of PAni and its derivatives can be protonated with a sufficiently strong acid due to the presence of basic sites (amine and imin groups) in the polymer structure.[13] Among polyaniline's derivations, poly (2-chloroaniline) (P2ClAn) shows better solubility and processibility but it has lower conductivity than that of PAni. The emeraldine salt (ES; protonated form of EB) is, however, the only electrically conducting form of the protonated forms of P2ClAn (Scheme 1).

Correspondence to: A. Gök (aysegul@fef.sdu.edu.tr).

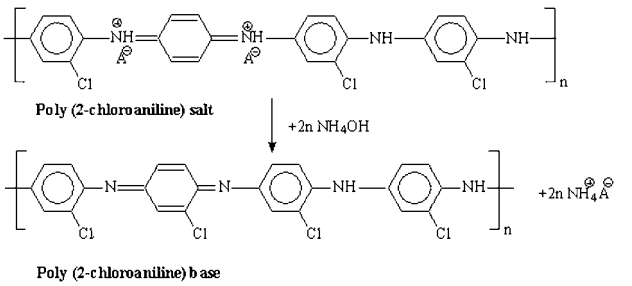

Scheme 1 The protonated emeraldine form of poly (2-chloroaniline) (one of the possible chemical representations) converts to poly(2-chloroaniline) deprotonated after the deprotonation in the alkaline media; e.g., in ammonium hydroxide solutions. A^- represents an arbitrary anion, e.g., chloride.

UV–vis spectroscopy is one of the mostly adopted techniques in characterizing the structures of PAni and its derivatives,[14] for its convenience[15] as compared with X-ray photoelectron spectroscopy,[16] etc. The UV–vis spectrum of PAni, which is one of the most studied conducting polymers, in deprotonated form is dominated by two absorption peaks at ~320 nm (Band I) and ~610 nm (Band II), respectively. Band I often assigned to $\pi \rightarrow \pi^*$ transition in benzenoid structure.[17] The absorption in the visible range, i.e., Band II, is ascribed to excision formation in the quinonoid rings.[18]

The intensity ratio of Band II to Band I (I_2/I_1) indicates the relative amount of quinoid diimine unit in PAni molecules, viz the oxidation state of PAni,[19,20] which plays a key role in determining the property of PAni. To date, UV–vis spectroscopy is still being used by many researchers in characterizing the oxidation state of PAni.[21,22]

Incorporation of inorganic nanoclusters into polymer matrices can dramatically improve their processability.[7,23,24] Although there are so many candidates as the polymeric matrix, one particular interest is the integration of inorganic nanoclusters with conducting polymers because the resulting nanocomposites may possess unique electrical and optical properties. Because of these properties, such materials are expected to find applications in electrochromic devices, nonlinear optical system, and photoelectrochemical devices.

Here, we selected PClAn as polymeric matrix because it has better solubility than polyaniline.[25] P2ClAn/SiO_2 composite was synthesized using SiO_2 to modify properties of P2ClAn. To clarify optical properties of composite, detail UV–vis study was done using different solvents. We present the effects of the solution concentration and solvent type on UV–vis spectroscopy for both P2ClAn and P2ClAn/SiO_2 using their protonated, deprotonated, and reprotonated forms. P2ClAn/SiO_2 composite is novel and its properties were compared with that of P2ClAn. We used three different solvents, DMF, NMP, and H_2SO_4. The preparation, characterization, and property evaluation of P2ClAn/SiO_2 composites are highlighted by different techniques in this article.

EXPERIMENTAL

Materials

2-Chloroaniline was purified by distillation at reduced pressure before use. SiO_2 (silica, 99.8%, Cat No: 381268) was received from Aldrich and it has particle size of 0.007 μm. Ammonium peroxydisulfate (APS), ammonia solution, sulfuric acid, hydrochloric acid, *N*,*N*-dimethyl formamide (DMP), *N*-methylpyrrolidone, and 2-chloroaniline were purchased from Aldrich.

Polymerization of 2-chloroaniline

Polymerizations were carried out in a 250-mL three-necked round bottom flask equipped with magnetic stirring. Typical recipies are described as follows: 2-chloroaniline was dissolved in 1*M* HCl aqueous solution. The solution was cooled down to 5°C and a solution of APS, with $n_{monomer}/n_{oxidant} = 2$, was added dropwise. Polymerization was carried out under nitrogen and controlled stirring for 24 h. At the end of polymerization, poly(2-chloroaniline) was filtered and washed with 1*M* HCl solution and distilled water before to be dried overnight at 60°C under vacuum.

Synthesis of P2ClAn/SiO_2 nanocomposite

P2ClAn/SiO_2 nanocomposite was prepared by "*in situ*" deposition oxidative polymerization of 2-chloroaniline hydrochloride using APS as oxidant in the presence of SiO_2 powders cooled by an ice bath. Before adding aqueous solution of APS, the suspension of SiO_2 and monomer solution was mixed to obtain a homogenous dispersion. The aqueous solution of APS was slowly added dropwise with vigorous stirring. The precipitated composite powder was filtered and washed with HCl solution and distilled water till the filtrate become colorless to remove the by-product, excess monomer, and oligomer and dried overnight at 60°C under vacuum. The amount of SiO_2 in nanocomposite was calculated as 20%.

The resulting P2ClAn and P2ClAn/SiO_2 emeraldine salts were converted into its deprotonated form (P2ClAn(EB)/SiO_2) by treating with 1*M* ammonium hydroxide solution. The deprotonated form of homopolymer and its composite were thoroughly washed with distilled water, and then vacuum-dried to constant mass for use. After deprotonation process, samples were reprotonated using 1*M* HCl solution.

Characterization

Fourier transform infrared (FTIR) spectra were recorded between 400 and 4000 cm^{-1} from KBr pel-

lets on a Perkin-Elmer Spectrum BX FTIR system (Beaconsfield, Buckinghamshire, HP91QA, England). The direct current electrical conductivity of the protonated P2ClAn and P2ClAn/SiO_2 nanocomposite was measured by standard four-probe method. UV–vis spectra were recorded between 250 and 900 nm using a 1 cm path length quartz cuvette, and pure DMF, NMP, and H_2SO_4 solvents were used as the reference on a Perkin–Elmer Lambda 20 UV–vis spectrophotometer. Five testing solutions at appropriate concentrations from 0.01 to 0.05 g/L for subsequent spectroscopic studies were prepared by dissolving 0.005 g powders in predetermined volumes of DMF, NMP, and H_2SO_4. For SEM analysis, samples were sputter coated with gold layers and photographs were taken on a scanning electron microscope model Jeol 5600-LV Model Scanning (Tokyo, Japan). Particle diameter analysis was done by using Philips ESEM-FEG XL30 Model (FEI Company B606L, USA) environmental scanning electron microscopy Field Emission Gun instrument operating at 10 kV at low vacuum. The sample was mounted on a double-sided Silver cohesive sheet; no gold coating is needed. Thermal stability of P2ClAn and its nanocomposites with SiO_2 was investigated by Perkin–Elmer model thermal parametric analyzer (Beaconsfield, Buckinghamshire, HP91QA, England) with nitrogen (a pure gas) at a flow rate of 35 mL/min. Magnetic susceptibilities were measured using Magway MSB Mk1 Model (Sherwood Scientific) Gouy Scale, according to the procedure reported elsewhere.[4] X-ray diffraction studies were performed by using Philips X-ray diffractometer (LabX, Midland, Canada) with CuKα as radiation source.

RESULTS AND DISCUSSION

Figures 1(a)–1(c) present the FTIR spectra of P2ClAn (protonated), P2ClAn (deprotonated), and (reprotonated) forms. The main peaks at 1579 cm^{-1} and 1501–1500 cm^{-1} in the spectrum of P2ClAn protonated

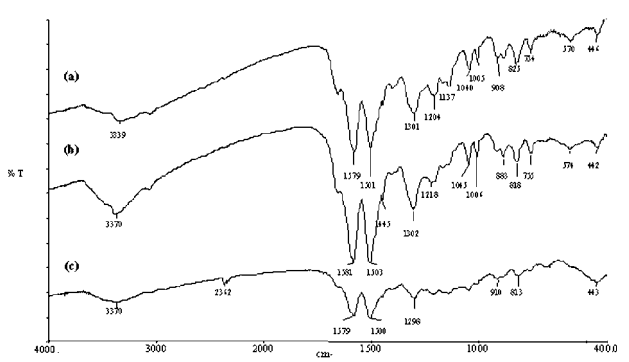

Figure 1 FTIR spectra of P2ClAn (a) protonated, (b) deprotonated, (c) reprotonated.

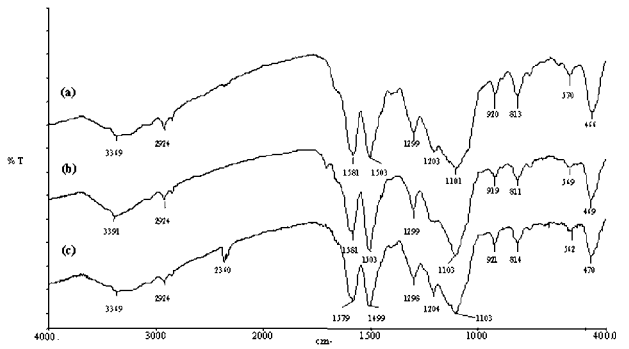

Figure 2 P2ClAn/SiO_2 (a) protonated, (b) deprotonated, (c) reprotonated.

and reprotonated forms correspond to quinone- and benzene-ring stretching deformations, respectively [Figs. 1(a) and 1(c)]. The 1137 cm^{-1} band is assigned to a vibration mode of the —NH^+— structure, which is formed during protonation.[26]

When P2ClAn are treated with an alkali, the green conducting emeraldine deprotonated (Scheme 1) 1579 and 1500 cm^{-1} modes in P2ClAn salts show a blue shift to 1581 and 1503 cm^{-1} in the P2ClAn deprotonated [Fig. 1(b)]. The 1302 cm^{-1} band is assigned to the C—N stretch of a secondary aromatic amine, whereas in the region of 1045–1006 cm^{-1}, the aromatic C—H in-plane bending modes are usually observed. Out-of-plane deformations of C—H on trisubstituted rings are located in the region of 883–818 cm^{-1}.[27] Additionally, it is seen that the intensity of band corresponding to quinoid ring at 1579 cm^{-1} has decreased in emeraldine deprotonated form [Fig. 1(b)].

The spectra of the P2ClAn/SiO_2 nanocomposite in the presence of SiO_2 [Figs. 2(a)–2(c)] differ from the spectra of P2ClAn forms. In the case of P2ClAn/SiO_2 nanocomposite, the additional peaks at 1100 and 466 cm^{-1} (characteristic of SiO_2) appeared.[20] It is well known that in systems with polyaniline, strong guest–host interactions, such as hydrogen bonding, occur in the form of NH. . .nanomatrix.[28] In P2ClAn/SiO_2 structure, there is H-bonding interactions in form of N—H. . .O—Si— between P2ClAn and SiO_2. These interactions have also been supported from shifting values in FTIR spectra. When P2ClAn/SiO_2 is treated with NH_4OH, band at 1203 cm^{-1} disappeared [Fig. 2(b)]. The intensities of the quinonoid band (1581 cm^{-1}) and benzenoid band (1503 cm^{-1}) are near to each other in P2ClAn/SiO_2 protonated form. However, in the spectrum of P2ClAn/SiO_2 deprotonated form, the intensity of the quinonoid band decreases [Fig. 2(b)]. After the reprotonated process with HCl, its intensity increases according to deprotonated form of nanocomposite [Fig. 2(c)]. This indicates that the oxidation state of P2ClAn/SiO_2 salts is higher than that of P2ClAn/SiO_2 deprotonated.

UV–vis results

P2ClAn and P2ClAn/SiO_2 in protonated, deprotonated, and reprotonated forms were solved into DMF, NMP, and H_2SO_4. Figures 3(a) and 3(b) show UV–vis spectra of P2ClAn and P2ClAn/SiO_2 deprotonated into NMP. As one can see, there are two major absorptions around 313–319 nm, which are related to the $\pi \rightarrow \pi^*$ transition in the benzenoid structure[29] and the absorption at the wavelength 596–630 nm, which is ascribed to excitation formation in the quinonoid rings.[30]

All samples into H_2SO_4 have shown three characteristic absorption bands 310–317, 520–536, and 748–813 nm. The first absorption is due to the excitation of the nitrogen in the benzonoid segments ($\pi \rightarrow \pi^*$ transition), while the second and the third ones are ascribed to polaron/bipolaron transition that occurs in protonated situation. All samples have shown two absorption bands into NMP and DMF whereas they exhibit three characteristic bands into H_2SO_4. NMP and DMF are basic enough to convert the protonated P2ClAn (ES) to the deprotonated P2ClAn (EB). However, all samples into H_2SO_4 show characteristic emeraldine salt forms. Hence they have three absorption bands showing characteristic of ES.

The intensities of both Band I and Band II of all samples decrease with decreasing concentration of the solutions in all solvents. Figures 4(a)–4(b) show the absolute values of the absorbance for the benzenoid structure (A_B) and quinonoid structure (A_Q) of protonated and deprotonoted of P2ClAn/SiO_2, i.e., the A_B and A_Q were plotted versus the concentration for all solvents.

It is evident that the concentration of the solution influences A_B more than it does A_Q, viz. A_B decreases faster than A_Q with decreasing concentration. Deprotonated forms of all samples have higher absorbance values than those of protonated forms for both benzenoid and quinoid units. This result shows that deprotonated forms of P2ClAn and P2ClAn/SiO_2 have better solubility than those of other forms.

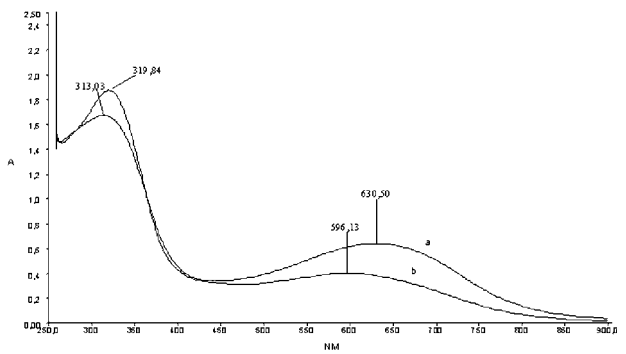

Figure 3 UV–vis spectra of (a) P2ClAn and (b) P2ClAn/SiO_2 deprotonated forms into NMP.

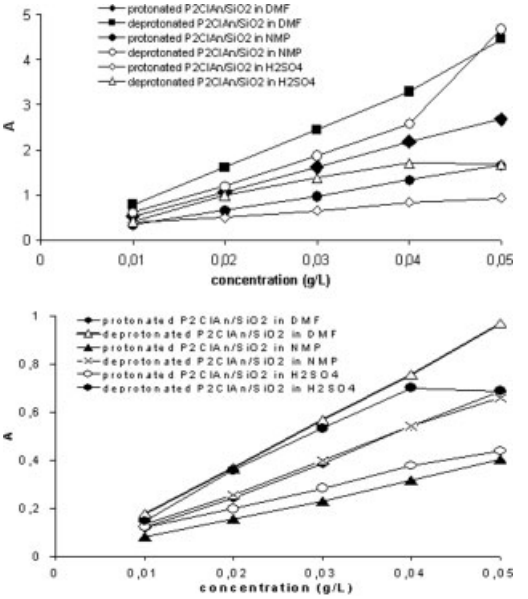

Figure 4 Absolute values of the absorbance for the benzenoid structure (a) and quinonoid structure (b) of protonated and deprotonated forms of P2ClAn/SiO_2.

The intensity ratio of A_Q/A_B were calculated from their UV–vis spectra. Figures 5(a)–5(f) correspond to A_Q/A_B values obtained for all forms of P2ClAn and P2ClAn/SiO_2 in various concentrations.

The ratio of intensities of A_Q/A_B is different from each into each solvent, especially into H_2SO_4. The intensity ratios of both P2ClAn and P2ClAn/SiO_2 show a decrease with increasing solution concentration into NMP whereas they have not changing too much value into DMF. In H_2SO_4 solvent, both the absorbance intensity of quinonoid and benzenoid rings have increased faster, and so the intensity ratio of A_Q/A_B into H_2SO_4 also increased as different from others. Moreover, the polaron band addition to the benzenoid and quinonoid bands was observed for all polymers into H_2SO_4 solvents. Here H_2SO_4 has doped polymer chain because λ_2 (nm), which contributed to polaron after doping and corresponded to localization of electron, shifted longer wavelength according to other solvents.

Table I shows maximum absorbance wavelengths of protonated, deprotonated, and reprotonated of P2ClAn and P2ClAn/SiO_2 (0.03 g/L) into all solvents. As can be seen from Table I, λ_2 (nm) for P2ClAn/SiO_2 nanocomposite has shifted to shorter wavelength in its protonated, deprotonated, and reprotonated forms into DMF, NMP, and H_2SO_4.

TGA results

The thermal stability of P2ClAn/SiO_2 composite has been investigated using thermogravimetric analysis. Figures 6(a)–6(c) depict the thermograms of SiO_2,

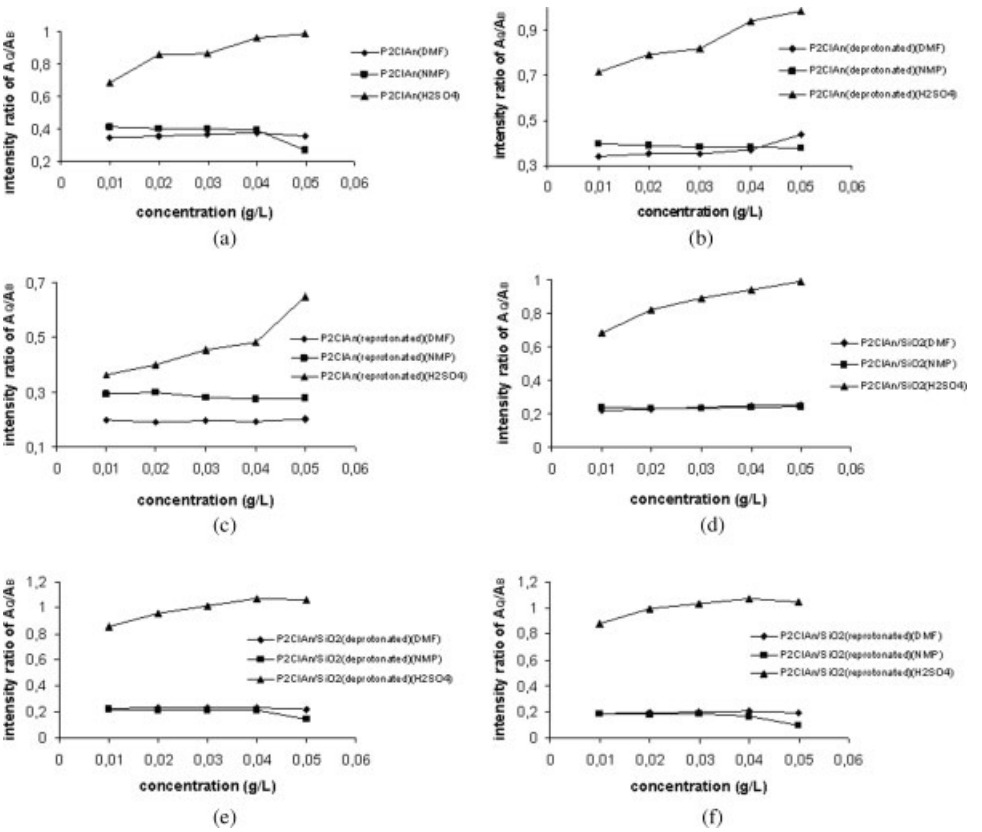

Figure 5 Intensity ratio of A_Q/A_B for all forms of P2ClAn and P2ClAn/SiO_2 into three solvents. (a) Protonated P2ClAn, (b) deprotonated P2ClAn, (c) reprotonated P2ClAn, (d) protonated P2ClAn/SiO_2, (e) deprotonated P2ClAn/SiO_2, (f) deprotonated P2ClAn/SiO_2.

P2ClAn, and P2ClAn/SiO_2, respectively. As indicated in the recent report[31] the onset decomposition temperatures of nanocomposites are higher than that of polymer and shifted towards the higher temperature range as the content of inorganic matrix. The decomposition temperatures obtained from thermograms are listed Table II. Initial decomposition temperatures confirm the increased thermal stability of

TABLE I
Maximum Absorbance Wavelengths of Protonated, Deprotonated, and Reprotonated of P2ClAn and P2ClAn/SiO_2 into All Solvents

Sample	Structure	Solvent	λ_1 (nm)	λ_2 (nm)	λ_3 (nm)
P2ClAn	Protonated	DMF	274	589	–
P2ClAn/SiO_2	Protonated	DMF	314	566	–
P2ClAn	Deprotonated	DMF	311	596	–
P2ClAn/SiO_2	Deprotonated	DMF	318	567	–
P2ClAn	Reprotonated	DMF	318	571	–
P2ClAn/SiO_2	Reprotonated	DMF	318	558	–
P2ClAn	Protonated	NMP	308	623	–
P2ClAn/SiO_2	Protonated	NMP	318	611	–
P2ClAn	Deprotonated	NMP	313	630	–
P2ClAn/SiO_2	Deprotonated	NMP	319	596	–
P2ClAn	Reprotonated	NMP	324	636	–
P2ClAn/SiO_2	Reprotonated	NMP	318	572	–
P2ClAn	Protonated	H_2SO_4	313	534	744
P2ClAn/SiO_2	Protonated	H_2SO_4	314	521	788
P2ClAn	Deprotonated	H_2SO_4	315	534	758
P2ClAn/SiO_2	Deprotonated	H_2SO_4	316	521	787
P2ClAn	Reprotonated	H_2SO_4	317	534	779
P2ClAn/SiO_2	Reprotonated	H_2SO_4	315	522	785

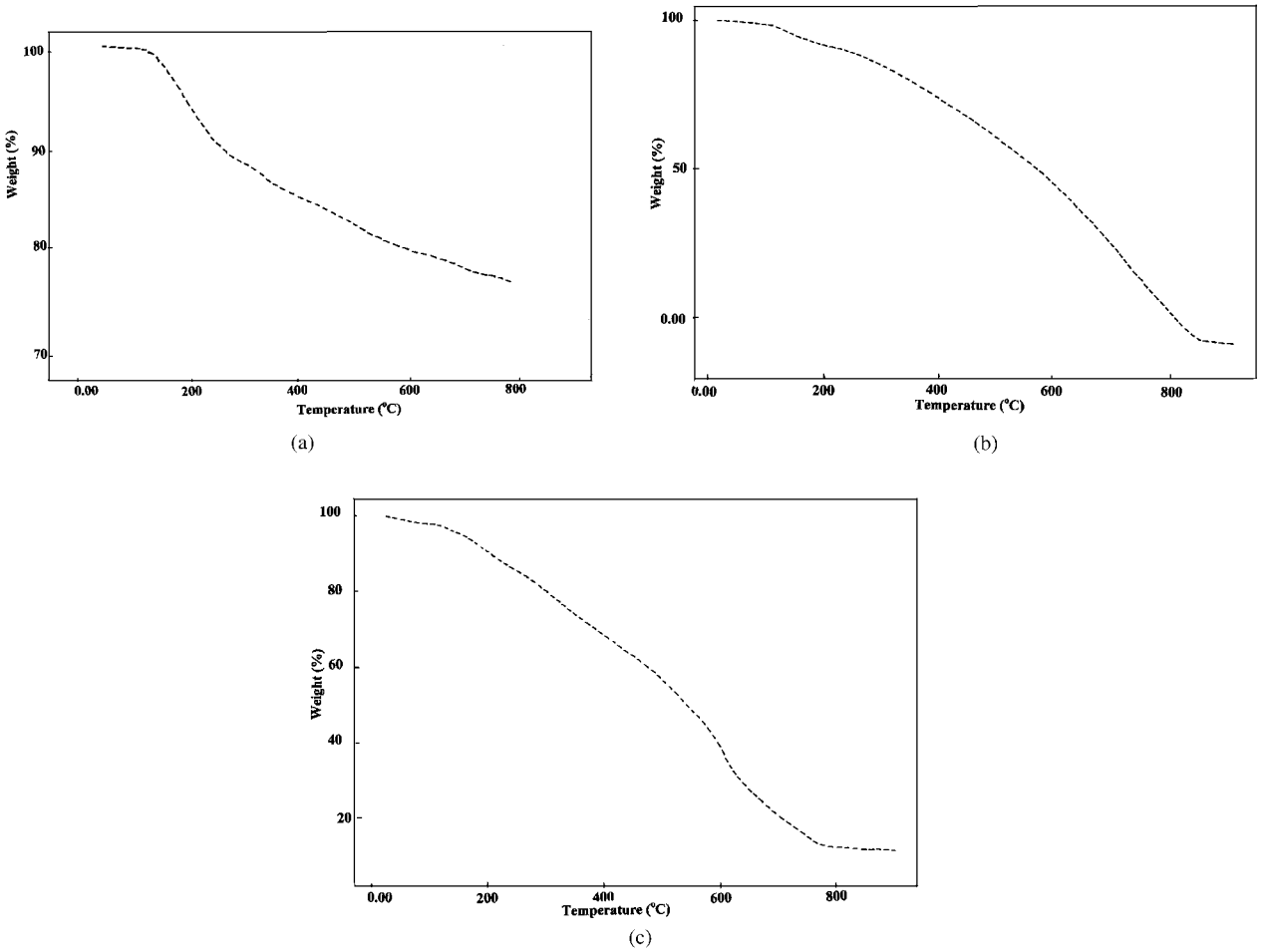

Figure 6 TGA curve of (a) SiO_2, (b) P2ClAn, (c) P2ClAn/SiO_2.

composite. Also, the residual weight of composites is much higher than that of P2ClAn. Thus, these data readily exhibited the enhanced thermogravimetric stability for the P2ClAn/SiO_2 composite relative to P2ClAn.

X-ray results

Crystallinity and orientation of conducting polymer are of much interest because the more highly ordered systems could display a metallic-like conductive state. X-ray powder diffraction measurements exhibited that the pattern of as-received SiO_2 [Fig. 7(a)] is typical for SiO_2.[32] The pure P2ClAn has typical pattern [Fig. 7(b)] for amorphous conducting polymer.[33] The X-ray diffraction pattern of P2ClAn/SiO_2 composite is shown in Figure 7(c). It has similar profile as observed in pure P2ClAn, indicating that the crystal structure of SiO_2 was not modified by P2ClAn. Also, these results indicate that P2ClAn is amorphous in the nanocomposite, which suggests that the addition of SiO_2 nanoparticles impedes the crystallization of the P2ClAn molecular chain. When P2ClAn is absorbed on the surface of the SiO_2 nanoparticles, the molecular chain of the absorbed P2ClAn is confined, and the degree of crystallinity decreases.[34]

SEM and ESEM—conductivity, magnetic susceptibility results

The compatibility between the organic polymer and silica has a great effect on the thermal, mechanical, and optical properties of the hybrid materials. Figure 8(a) shows the SEM images of the as-received SiO_2. It can be seen that SiO_2 are spherical and diameter of particle is at nanometer level. In the SEM photography, aggregation of silica was not observed. The fracture surface was very dense. P2ClAn shows particular morphology which is relatively uniform

TABLE II
Thermal Degradation Temperatures of Samples

Sample	T_i^* (°C)	T_m (°C)	T_f (°C)	Residue % at 800°C
SiO_2	154	490	822	75
P2ClAn	111	476	835	0
P2ClAn/SiO_2	155	468	778	10

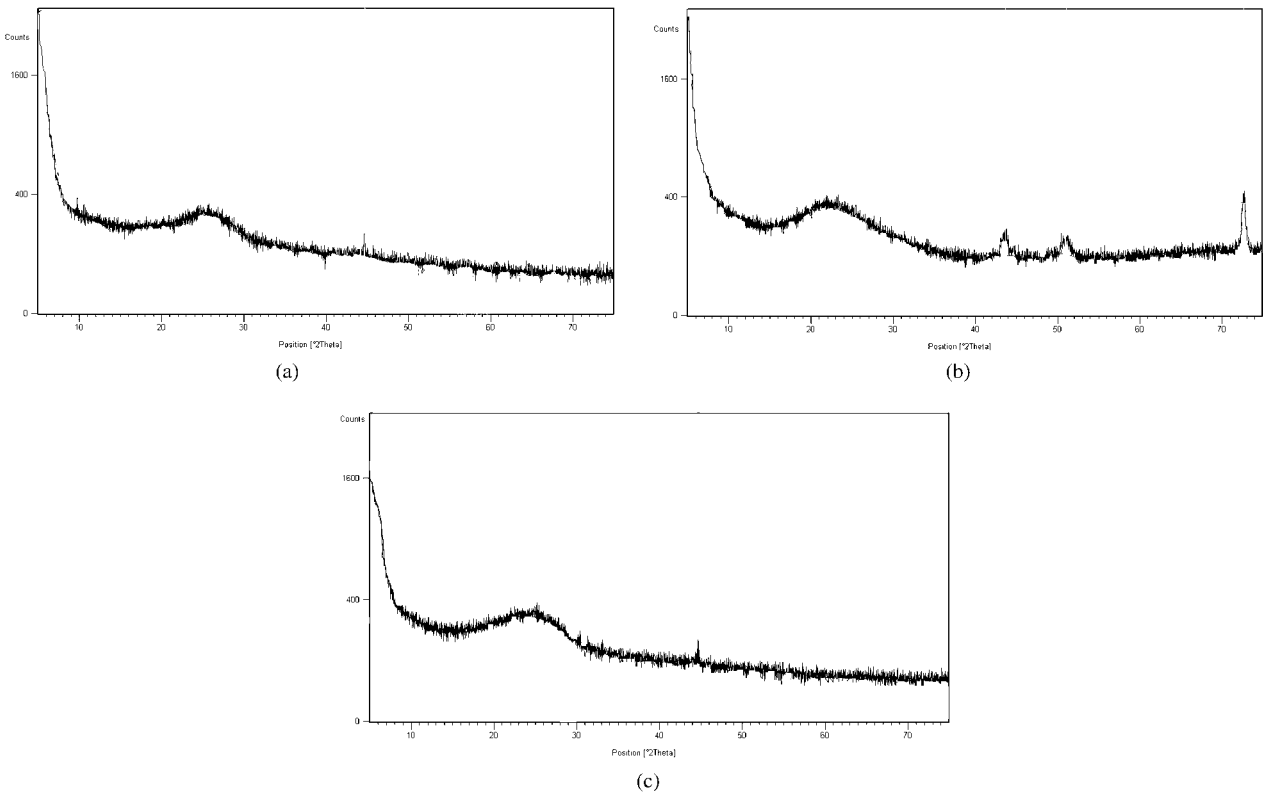

Figure 7 XRD pattern of (a) P2ClAn, (b) SiO_2, (c) P2ClAn/SiO_2.

[Fig. 8(b)]. After *in situ* polymerization reaction, P2ClAn/SiO_2 composite indicates that SiO_2 particles have a nucleus effect and caused a homogeneous structure in composite [Fig. 8(e)]. P2ClAn was preferentially formed on the surfaces of the SiO_2 particles during chemical oxidative polymerization of 2ClAn in the presence of the particles, resulting in core–shell structured composite particles. The dimension and morphology of SiO_2 changed after polymerization of 2ClAn onto SiO_2 surface. The SiO_2 particles would be present not only on composite particles surface but also distributed through their interior, a situation quite similar to that reported elsewhere.[10,12] The dispersion of the silica in the polymer matrix was also observed with ESEM. It can be seen from ESEM image (Fig. 9) that P2ClAn/SiO_2 composite has diameter of less than 1 μm. Additionally, the surface morphologies of P2ClAn and P2ClAn/SiO_2 were investigated with SEM after protonated, deprotonoted, and reprotonoted processes, respectively [Figs. 8(d)–8(g)].

After reprotonated process of P2ClAn, dimensions of granules have increased than that of P2ClAn deprotonated. The similar change has been observed in the structure of P2ClAn/SiO_2 composites. As can be seen from Figure 8(c), P2ClAn/SiO_2 reprotonated have bigger granular dimensions than its deprotonated structure [Fig. 8(b)].

The electrical conductivity of the P2ClAn and P2ClAn/SiO_2 were described as 4.6×10^{-7} and 1.3×10^{-5} S cm^{-1}. The conductivity of the P2ClAn/SiO_2 composite is higher than that of P2ClAn. Similar phenomenon was also found for PAni/TiO_2, PAni/WO_3, and PAni/clay composites.[8,11,35] The increase in conductivity would be due to the increase of efficiency of charge transfer between SiO_2 and polymer chains. SiO_2 might be increase protonation effect of polymer. Moreover, UV–vis results of all samples into H_2SO_4 solvent exhibited that for P2ClAn/SiO_2, λ_3 value leads to increase of conjugation length and brings about the increase of conductivity. Protonation in P2ClAn/SiO_2 would lead to the formation of radical cations by an internal redox reaction, causing reorganization of electronic structure to produce semiquinone radical cations, and accordingly the conductivity would be enhanced. Also, SEM images showed that P2ClAn/SiO_2 composite has homogenous morphology supporting good conductivity.

The magnetic properties of the composites have been considered by measuring magnetic susceptibility. The mass susceptibility values of samples were calculated from Gouy balance measurements. The mass susceptibility values of P2ClAn, SiO_2 and P2ClAn/SiO_2 are (+) 3.25×10^{-9}, (−) 4.00×10^{-9}, and (+) 3.6×10^{-9} (SI). SiO_2 has diamagnetic prop-

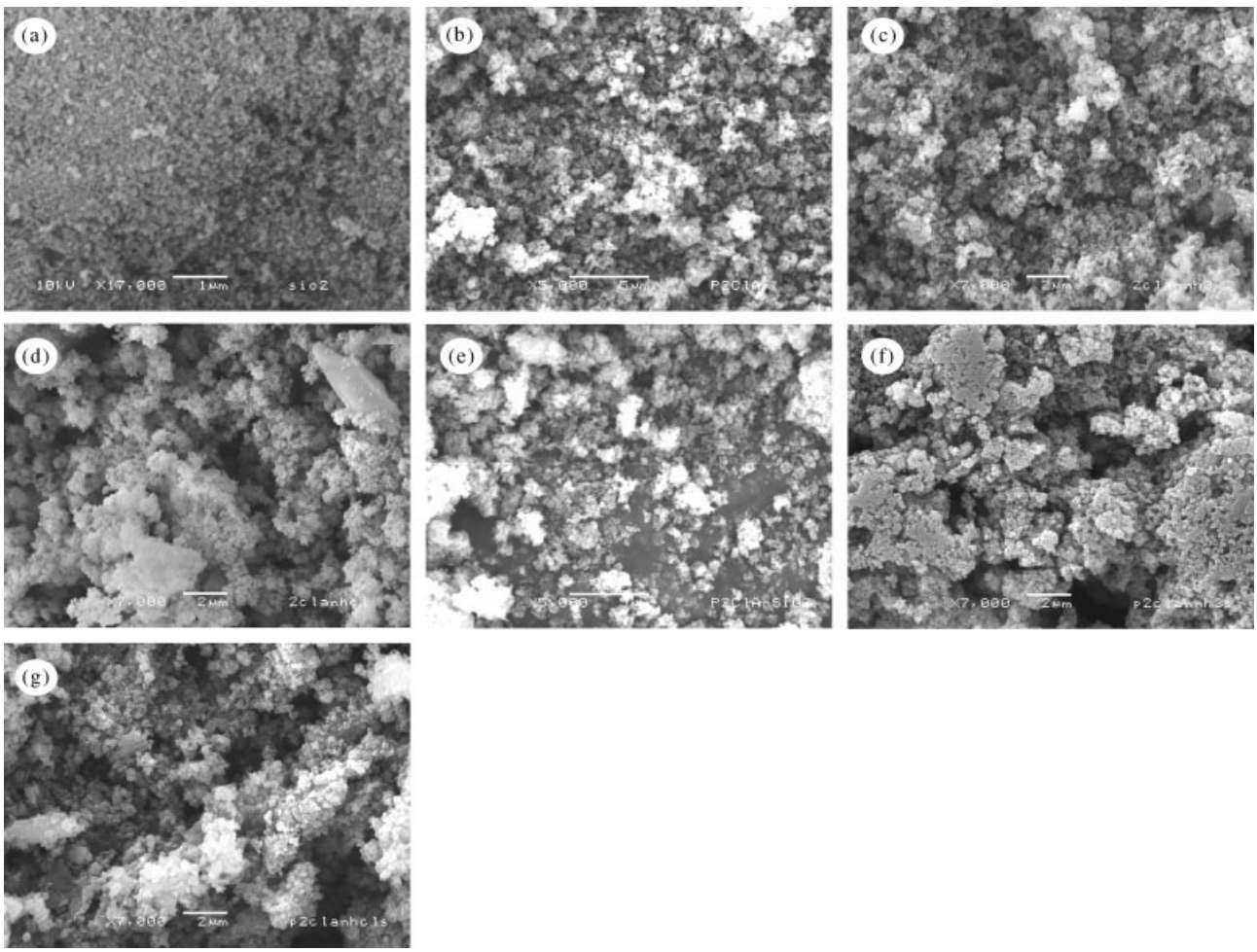

Figure 8 SEM micrographs of (a) SiO_2, (b) protonated P2ClAn, (c) deprotonated P2ClAn, (d) reprotonated P2ClAn, (e) protonated P2ClAn/SiO_2, (f) deprotonated P2ClAn/SiO_2, (g) deprotonated P2ClAn/SiO_2.

erties. P2ClAn/SiO_2 nanocomposite shows mass susceptibility similar to that of P2ClAn due to P2ClAn absorbed on the surface of the SiO_2 nanoparticles. These results are compatible with results of X-ray. The charge carriers in composite produced upon doping are single charged polarons with spin ½, which are the origin of magnetic susceptibility.[36]

CONCLUSIONS

P2ClAn and P2ClAn/SiO_2 were synthesized by *in situ* chemical oxidative polymerization method using $(NH_4)_2S_2O_8$ oxidant. The conductivity of composite can be designed to be higher than that of P2ClAn. The TGA results confirm the enhanced thermal stability relative to P2ClAn. UV–vis properties of P2ClAn and P2ClAn/SiO_2 composite were investigated into three different solvents. Their protonated, deprotonated and reprotonated forms were used for UV–vis measurements. They exhibited interesting properties both in their all forms and solvents. The changes in optical spectra had to be considered if practical applications of such materials are envisaged. P2ClAn/SiO_2 exhibited a better thermal stability regarding to P2ClAn. The conductivity and solu-

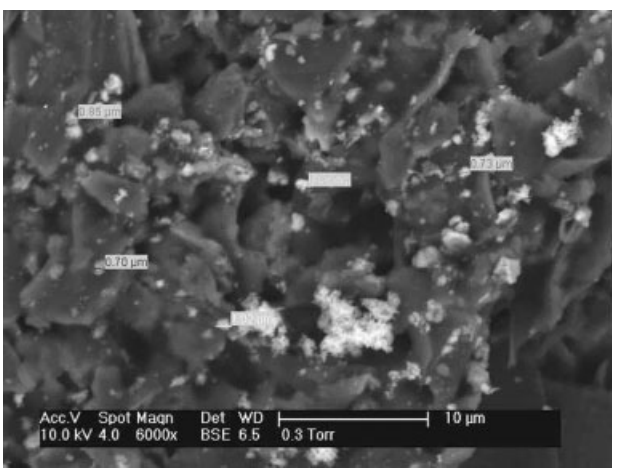

Figure 9 ESEM micrograph of P2ClAn/SiO_2.

bility of P2ClAn were increased preparing P2ClAn/SiO_2. Such processible composites will be promising candidates for advanced materials to be used in the high technology industries in the future.

References

1. Anand, J.; Palaniappan, S.; Sathyanarnayana, D.N. Prog Polym Sci 1998, 23, 993.
2. Erdem, E.; Karakışla, M.; Saçak, M. Eur Polym J 2004, 40, 785.
3. Tange, H.; Kitani, A.; Shiotani, M. Electrochim Acta 1996, 41, 1561.
4. Gök, A.; Sarı, B. J Appl Polym Sci 2002, 84, 1993.
5. Kuwabata, S.; Masui, S.; Yoneyama, H. Electrochim Acta 1999, 44, 4593.
6. Liu, Y. J.; DeGroot, D.C.; Schindler, J. J.; Kannerwurf, C. R.; Kanatzidis, M. G. Adv Mater 1993, 5, 369.
7. Chandrakanthi, R. L. N.; Careem, M. A. Thin Solid Films 2002, 417, 51.
8. Nasciment, G. M.; Constantino, V. R. L.; Temperini, M. L. A. Macromolecules 2002, 35, 7535.
9. Tang, B. Z.; Geng, Y. H.; Lam, J. W. Y.; Li, B. S. Chem Mater 1999, 105, 99.
10. Biswas, M.; Ray, S. S.; Liu, Y. P. Synth Met 1999, 105, 99.
11. Su, S. J.; Kuramoto, N. Synth Met 2000, 114, 147.
12. Ray, S. S.; Biswas, M. Synth Met 2000, 108, 231.
13. Quillard, S.; Berrada, K.; Louarn, G.; Lefrant, S.; Lapkowski, M.; Pron, A. New J Chem 1995, 19, 365.
14. Albuquerque, J. E.; Mattoso, L. H. C.; Bclogh, D. T.; Ferra, R. M.; Masters, J. G.; MacDiarmid, A. G. Synth Met 2000, 113(1/2): 19.
15. Alexandre, M.; Dubois, P. Mater Sci Eng R Rep 2000, 28(1/2), 1.
16. Lankri, E.; Levi, M. D.; Gofer, Y.; Aurbach, D.; Otero, T. J Electrochem Soc 2002, 149, E204.
17. Wan, M. X. Synth Met 1989, 31, 51.
18. Monkmen, A. P. In Conjugated Polymeric Materials (Nato ASI Series E: Applied Sciences, Vol. 182); Bredes J. L., Chance, R. R., Eds.; Kluwer: Dordiecht, The Netherlands, 1990; p 273.
19. Wolf, J. F.; Forbes, C. E.; Gould, S.; Shacklette, L. W. J Electrochem Soc 1989, 136, 2887.
20. Wei, Y.; Hsueh, K. F.; Jang, G. W. Macromolecules 1994, 27, 518.
21. Linfors, T.; Ivaska, A. J Electroanal Chem 2002, 535, 65.
22. Chen, L.; Yu, Y.; Mao, H.; Lu, X.; Zhang, W.; Wie, Y. Synth Met 2005, 129, 134.
23. O'Regon, B.; Gratzel, M. Nature 1991, 353, 737.
24. Wang, V.; Herron, N. Chem PhysLett 1992, 200, 71.
25. Gök, A.; Sarı, B.; Talu, M. Synth Met 2004, 142, 41.
26. Chlang, J. C.; Macdiamid, A. G. Synth Met 1986, 13, 193.
27. Ping, Z. J Chem Soc Faraday Trans 1996, 92, 2063.
28. Lee, D.; Char, K.; Lee, S. W.; Park, Y. W. J Mater Chem 2003, 13, 2942.
29. Mattoso, L. H. C.; Manohar, S. K.; MacDiarmid, A. G.; Epstein, A. J Polym Sci Part A: Polym Chem 1995, 33, 1227.
30. Cao, Y.; Smith, P.; Heeger, A. J. Synth Met 1989, 32, 263.
31. Okamoto, M. J. Ind Eng Chem 2004, 10, 1156.
32. Hwang, S. T.; Hahn, Y. B.; Nahm, K. S.; Lee, Y. S. Colloids Surf A 2005, 259, 77.
33. Gök, A.; Kaplan Can, H.; Sarı, B.; Talu, M. Mater Sci 2005, 59, 80.
34. Hesheng, X.; Qi, W. Chem Mater 2002, 14, 2158.
35. Parvatikar, N.; Jain, S.; Khasim, S.; Revansiddappa, M.; Bhoraskar, S. V.; Ambika Prasad, M. V. N. Sens Actuators B Chemical 2006, 114, 359.
36. Petr, A.; Neudeek, A.; Dunsch, L. Chem Phys Lett 2005, 40, 130.